

## Electronic Supplementary Information

### Heterojunction double dumb-bell $\text{Ag}_2\text{Te}$ -Te- $\text{Ag}_2\text{Te}$ nanowires

Anirban Som *and* T. Pradeep\*

DST Unit of Nanoscience (DST-UNS), Department of Chemistry, Indian Institute of Technology Madras, Chennai - 600 036, India.

\*E-mail: [pradeep@iitm.ac.in](mailto:pradeep@iitm.ac.in)

#### Table of contents

Number	Description	Page No.
S1	Size distribution of Te and $\text{Ag}_2\text{Te}$ NWs	2
S2	HRTEM and XRD of Te and $\text{Ag}_2\text{Te}$ NWs, EDS of $\text{Ag}_2\text{Te}$ NWs	3
S3	TEM image and EDS of partially silver reacted Te and the biphasic NWs	4
S4	HRTEM, PXRD and solid state annealing data for partially silver reacted Te NWs	5
S5	Diameter distribution in the middle And end sections in dumb-bell shaped NWs, variation of diameter along a single dumb-bell shaped NW	6
S6	HRTEM images of heterojunction covering the NW diameter	7
S6	TEM images showing the time dependent growth of biphasic NWs	8
S7	EDS showing time dependent growth of biphasic NWs	9
S8	Bending and breaking of biphasic system on annealing	10
S9	Temperature dependence of the growth of biphasic NWs	11
S10	Tuning the length of Te and $\text{Ag}_2\text{Te}$ sections	12

## S1. Supporting information 1

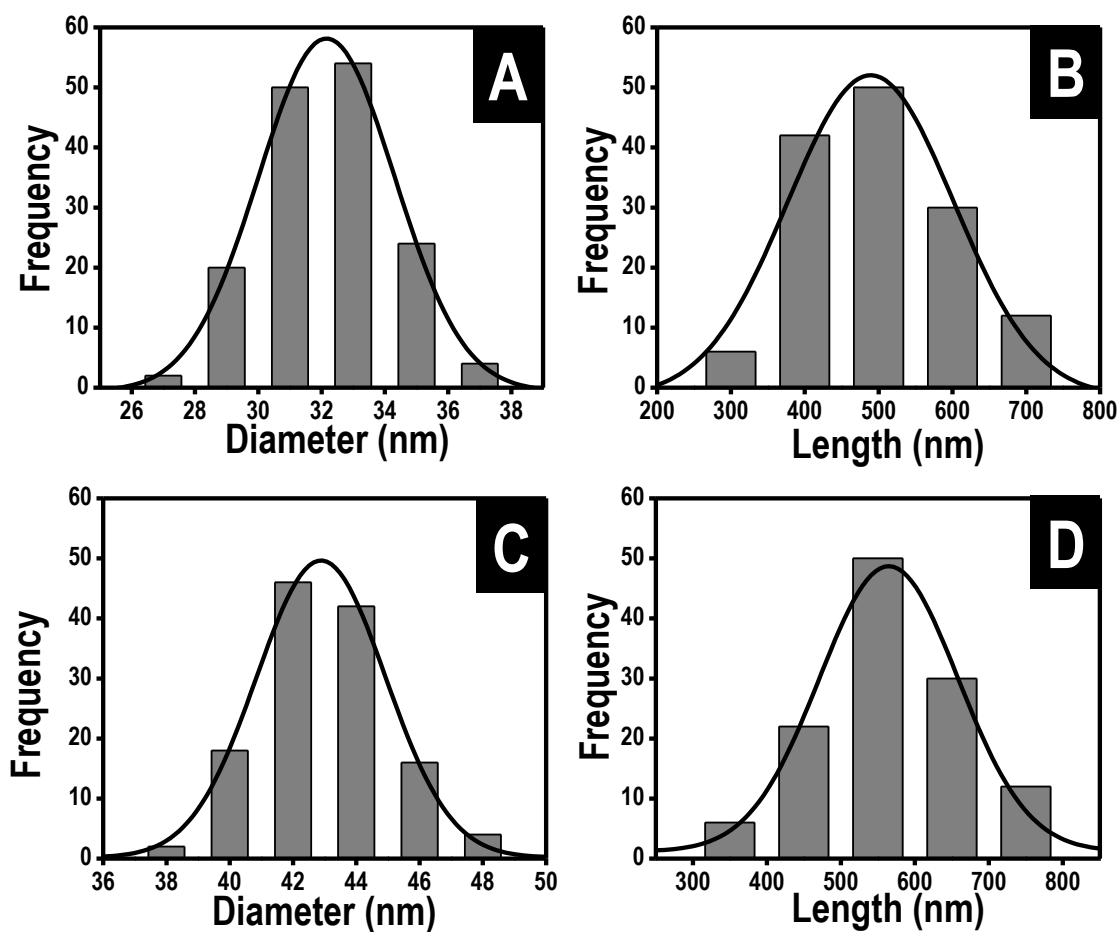


**Fig. S1** Size distribution of Te and Ag<sub>2</sub>Te NWs. (A) Diameter and (B) length distribution of Te NWs. (C) and (D) Corresponding distributions in Ag<sub>2</sub>Te NWs. Average length and diameter were 488 and 32.2 nm, respectively in Te NWs and 561 and 42.8 nm, respectively in Ag<sub>2</sub>Te NWs, which correspond to 15% increase in length and 33% increase in diameter upon chemical transformation.

## S2. Supporting information 2

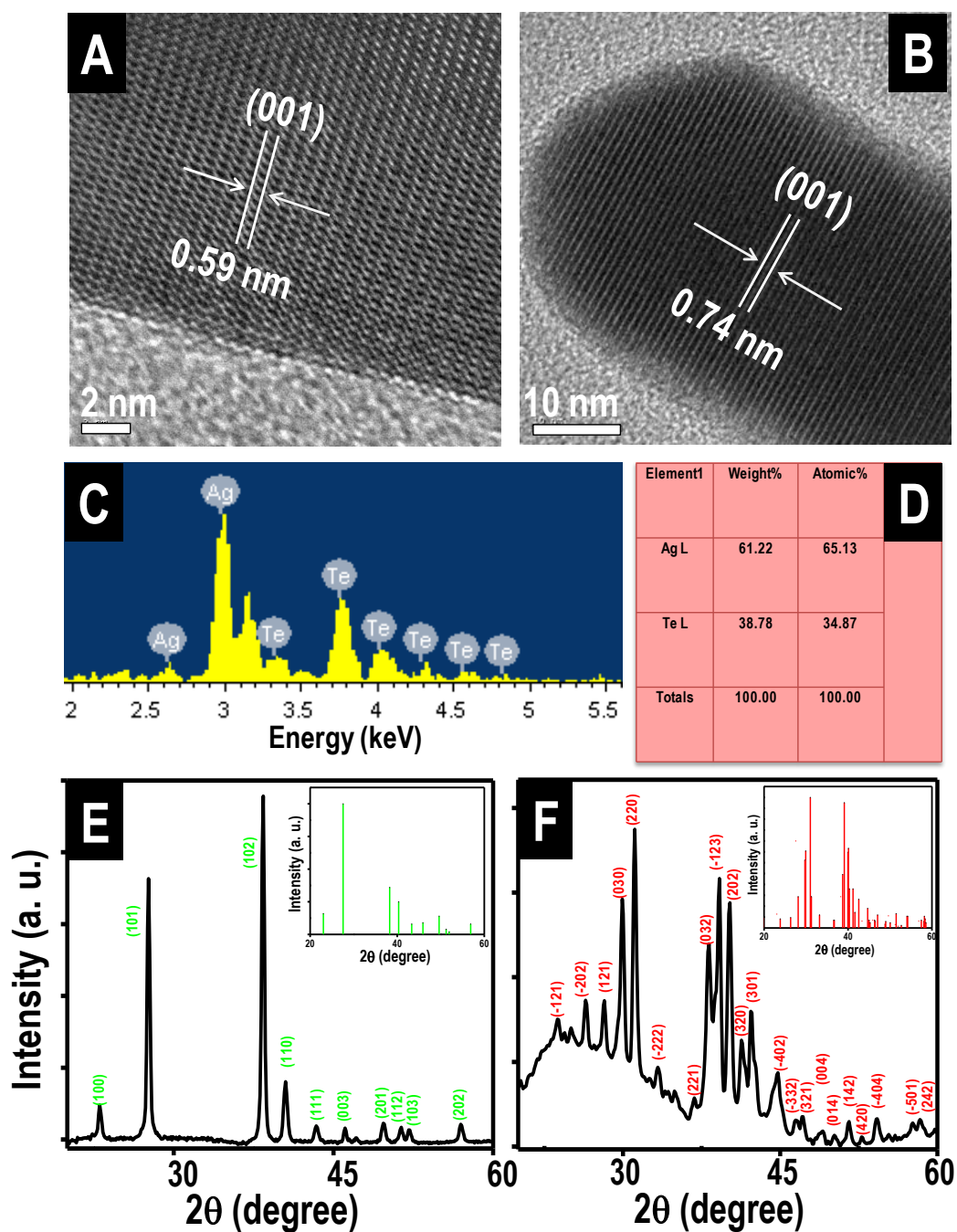


**Figure S2.** (A) Lattice resolved TEM image of a single hexagonal Te nanowire. (B) High resolution TEM image of a monoclinic  $\text{Ag}_2\text{Te}$  nanowire. (C) EDS spectrum of  $\text{Ag}_2\text{Te}$  nanowires showing the presence of both Ag and Te. (D) Elemental quantification corresponding to the spectrum, shows an atomic ratio of  $\sim 2:1$  for Ag and Te. (E) PXRD pattern of Te NWs. All the peaks are assigned to hexagonal phase of Te (JCPDS No. 36-1452). (F) PXRD pattern of  $\text{Ag}_2\text{Te}$  NWs. Pattern matches with the pattern of monoclinic phase of  $\text{Ag}_2\text{Te}$  (JCPDS No. 34-0142). Corresponding JCPDS patterns are shown in the insets of E and F.

### S3. Supporting information 3

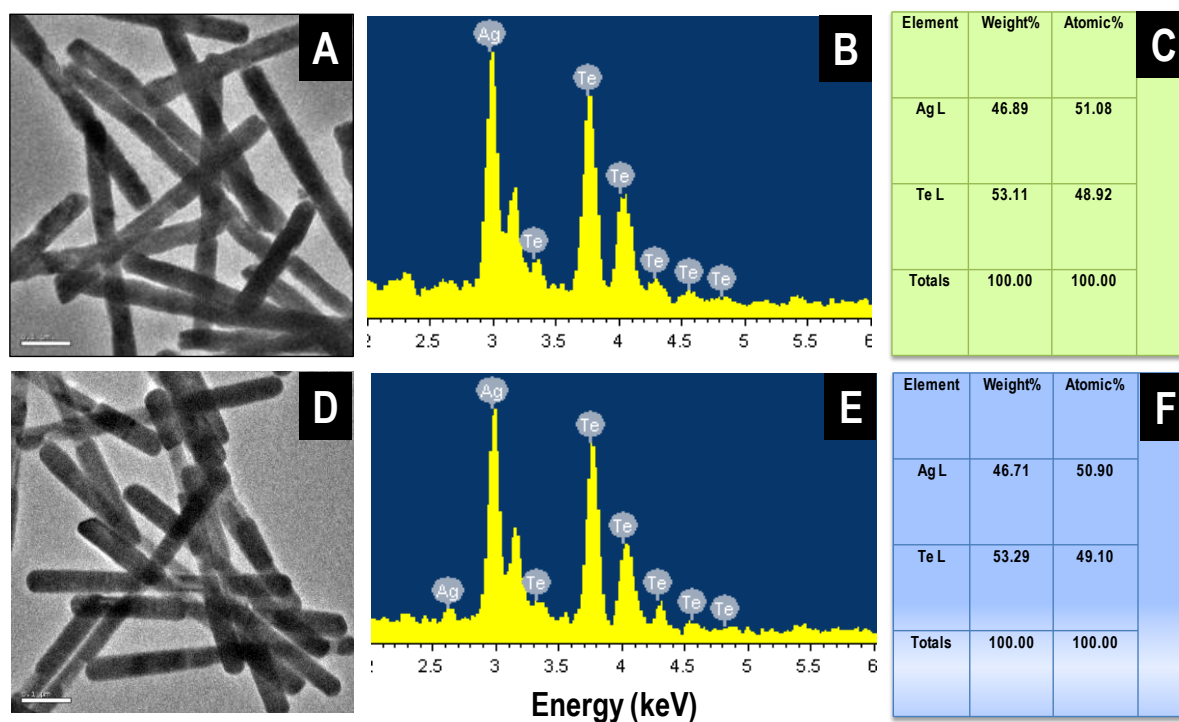


**Figure S3.** (A) Large area TEM image of partially silver reacted Te NWs. (B) EDS spectrum taken from the same area showing incorporation of silver in the nanowires. (C) EDS elemental quantification for Ag and Te in partially silver reacted Te nanowires. (D) Large area TEM image of phase segregated  $\text{Ag}_2\text{Te}$ -Te- $\text{Ag}_2\text{Te}$  nanowires. (E) EDS spectrum of  $\text{Ag}_2\text{Te}$ -Te- $\text{Ag}_2\text{Te}$  nanowires. (F) Quantification of total Ag and Te in  $\text{Ag}_2\text{Te}$ -Te- $\text{Ag}_2\text{Te}$  NWs. Both the NWs show similar Ag:Te ratio and indicates no silver loss during the annealing process in solution. Scale bar in both TEM images is 100 nm.

#### S4. Supporting information 4

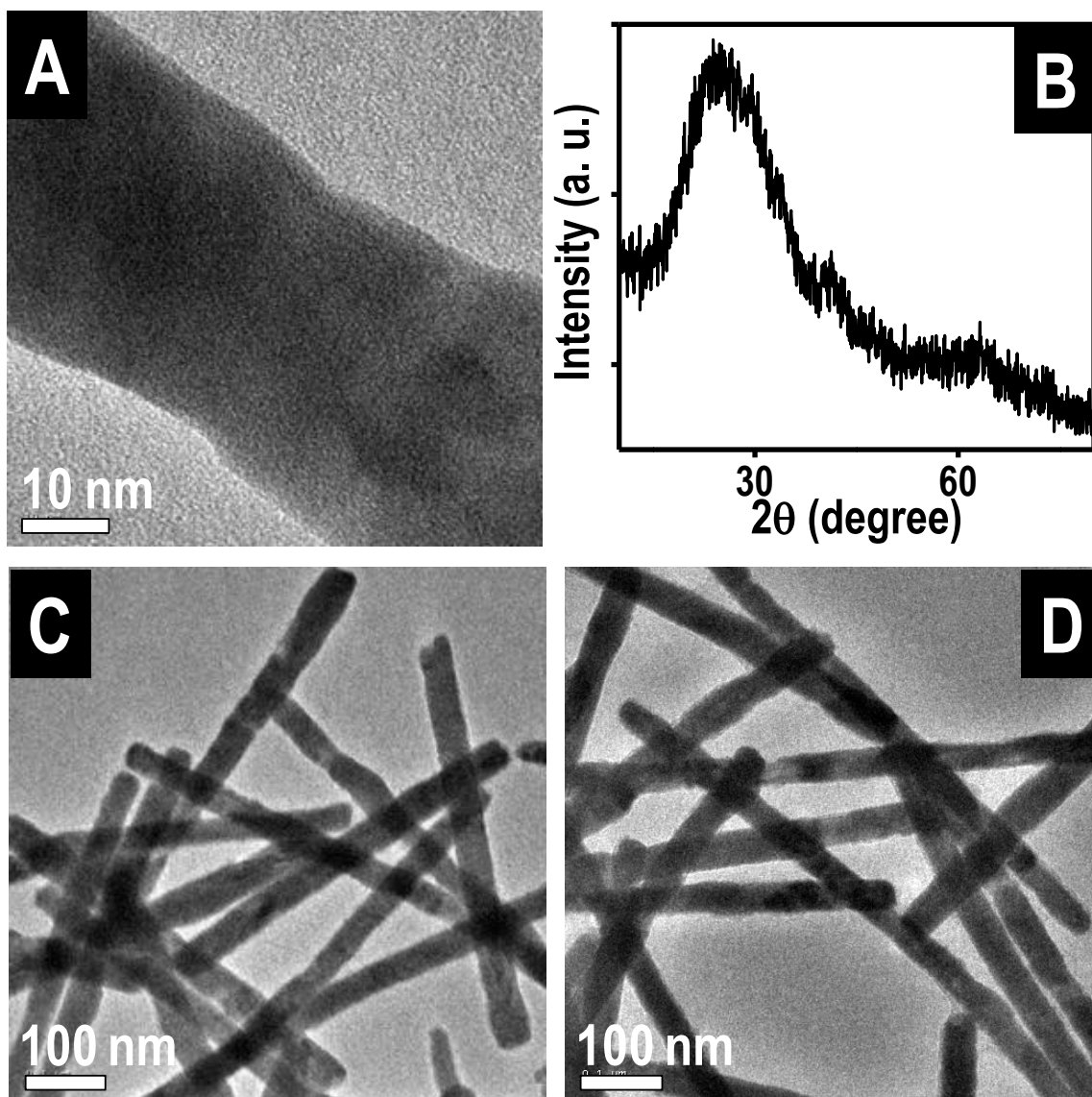


**Figure S4.** (A) High magnification TEM image of partially silver reacted Te nanowires. (B) XRD pattern of the partially silver reacted Te nanowires. Representative TEM images taken from these nanowires (C) before and (D) after solid state annealing at 75°C for 24 hours. Change in nanowire morphology was not observed.

## S5. Supporting information 5

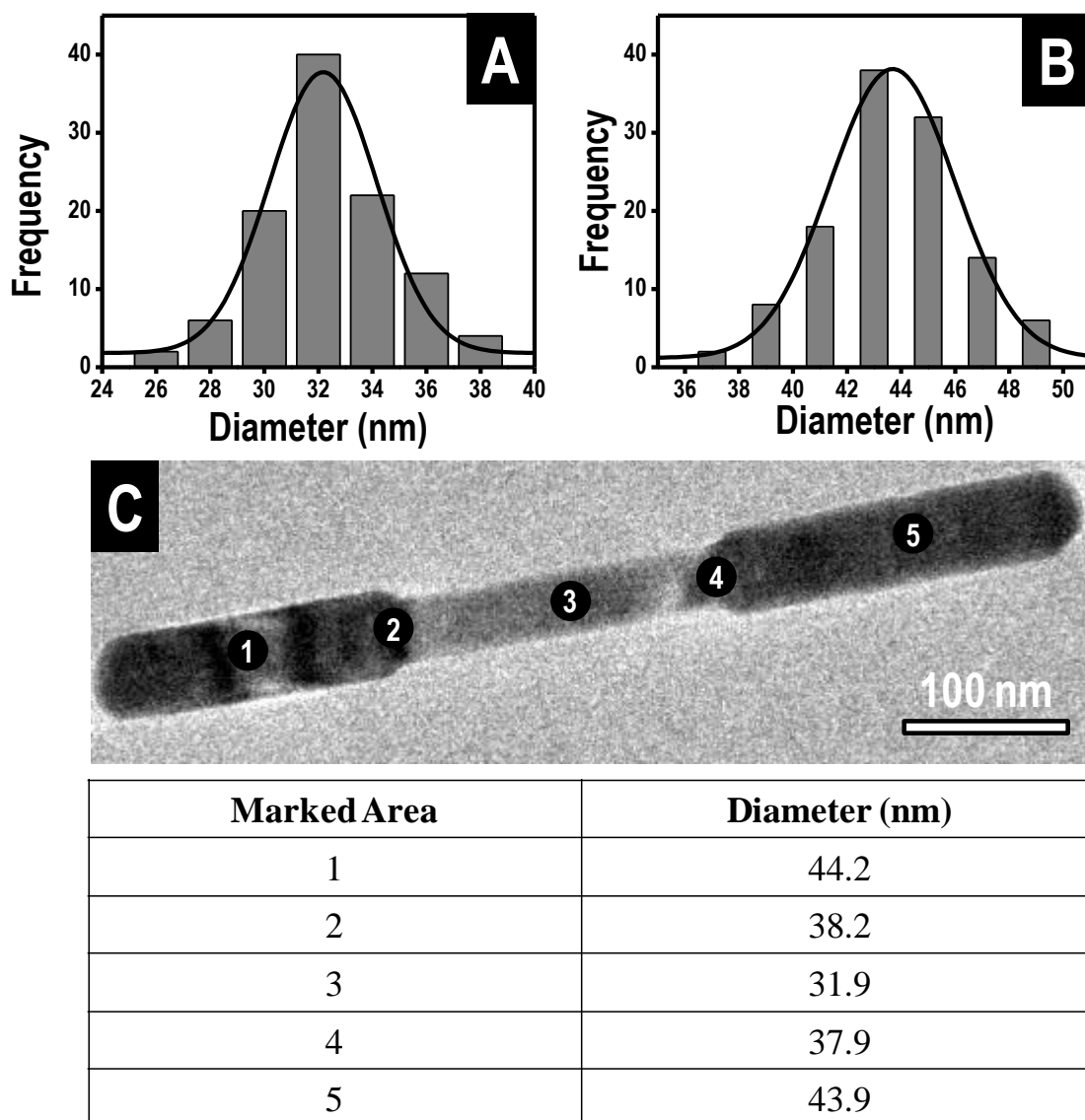


**Fig. S5** (A) Diameter distribution in the middle section of dumb-bell shaped NWs. (B) Diameter distribution in the two end segments of the NWs. (C) Variation of diameter across the length of a biphasic NW. Diameters from the marked areas are shown in a tabular form.

## S6. Supporting information 6

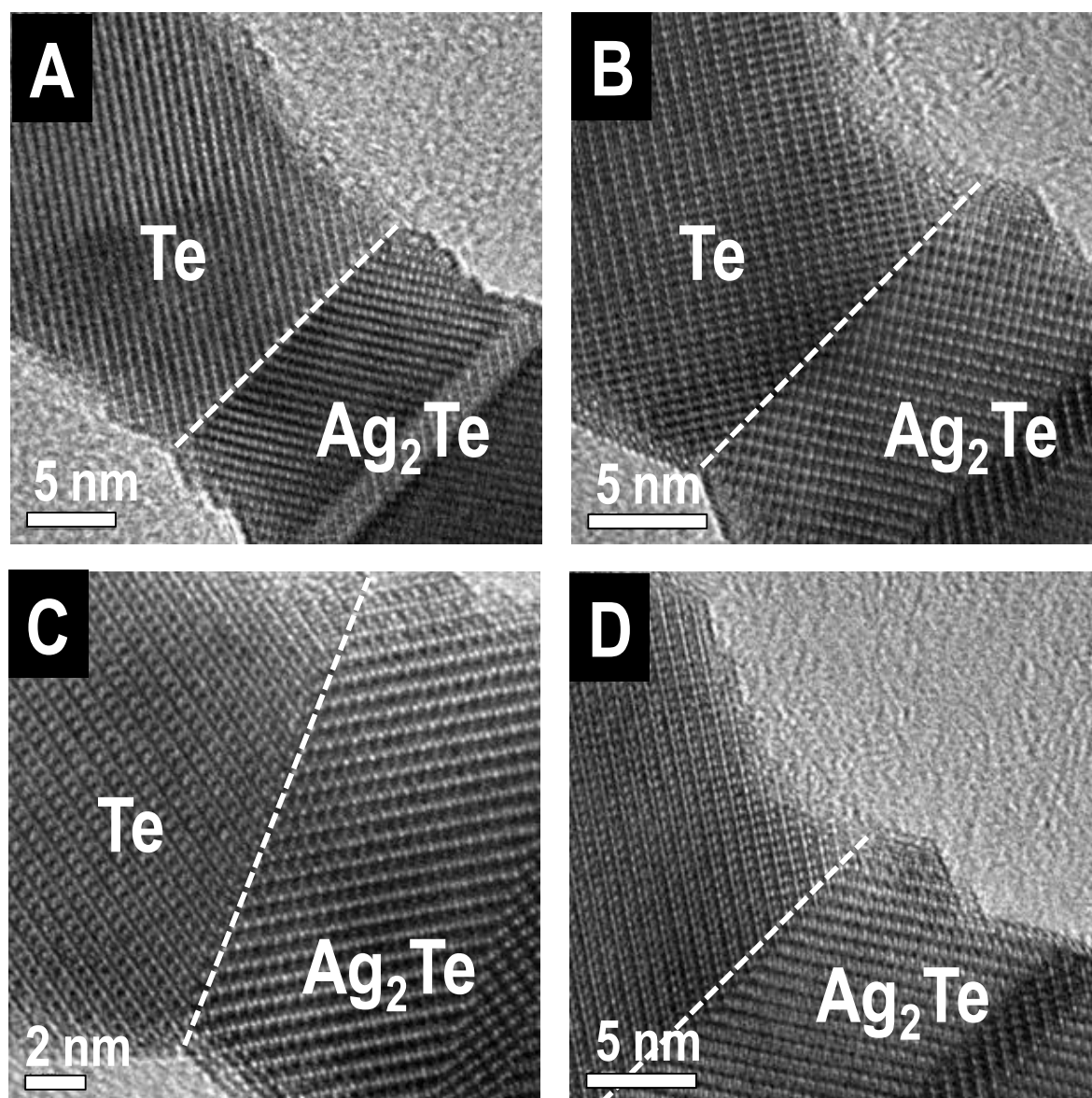


**Fig. S6** HRTEM images of the heterojunction shown in Fig. 3B. (A), (B) and (C) show HRTEM of the heterojunction covering the entire diameter of the NW at different magnifications. (D) HRTEM of other half of the NW (across the diameter).

### S7. Supporting information 7

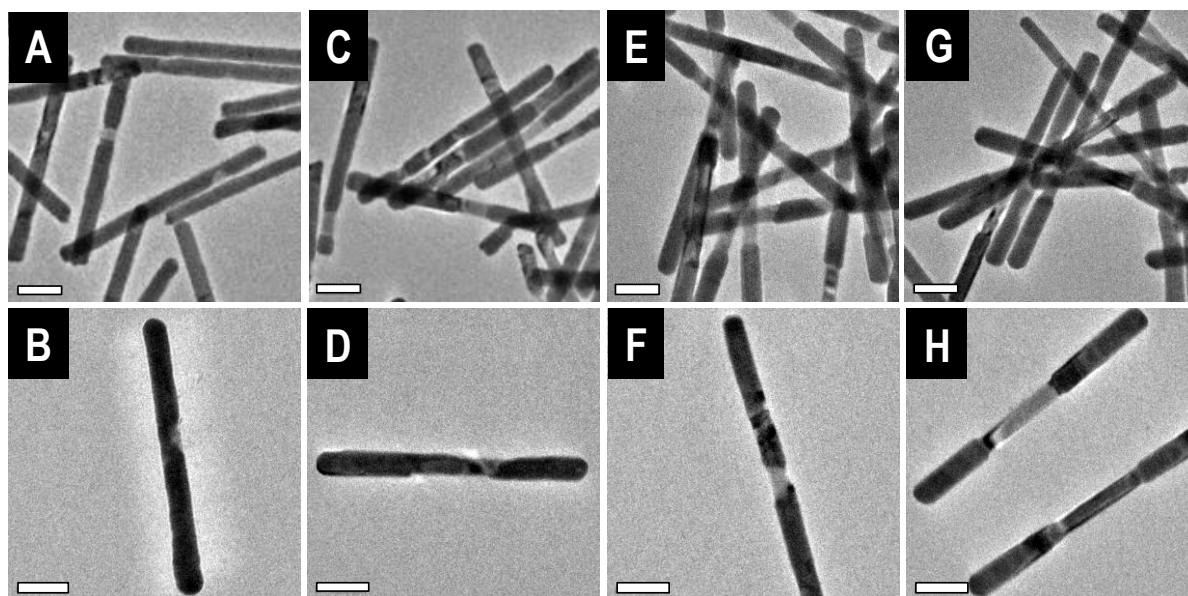


**Figure S7.** Morphological changes leading to biphasic dumb-bells during annealing of partially silver reacted Te nanowires. TEM images taken after (A,B) 6 h, (C,D) 12 h, (E,F) 18 h and (G,H) 24 h annealing treatment of the nanowires in solution. Scale bar is 100 nm in all the images.

## S8. Supporting information 8

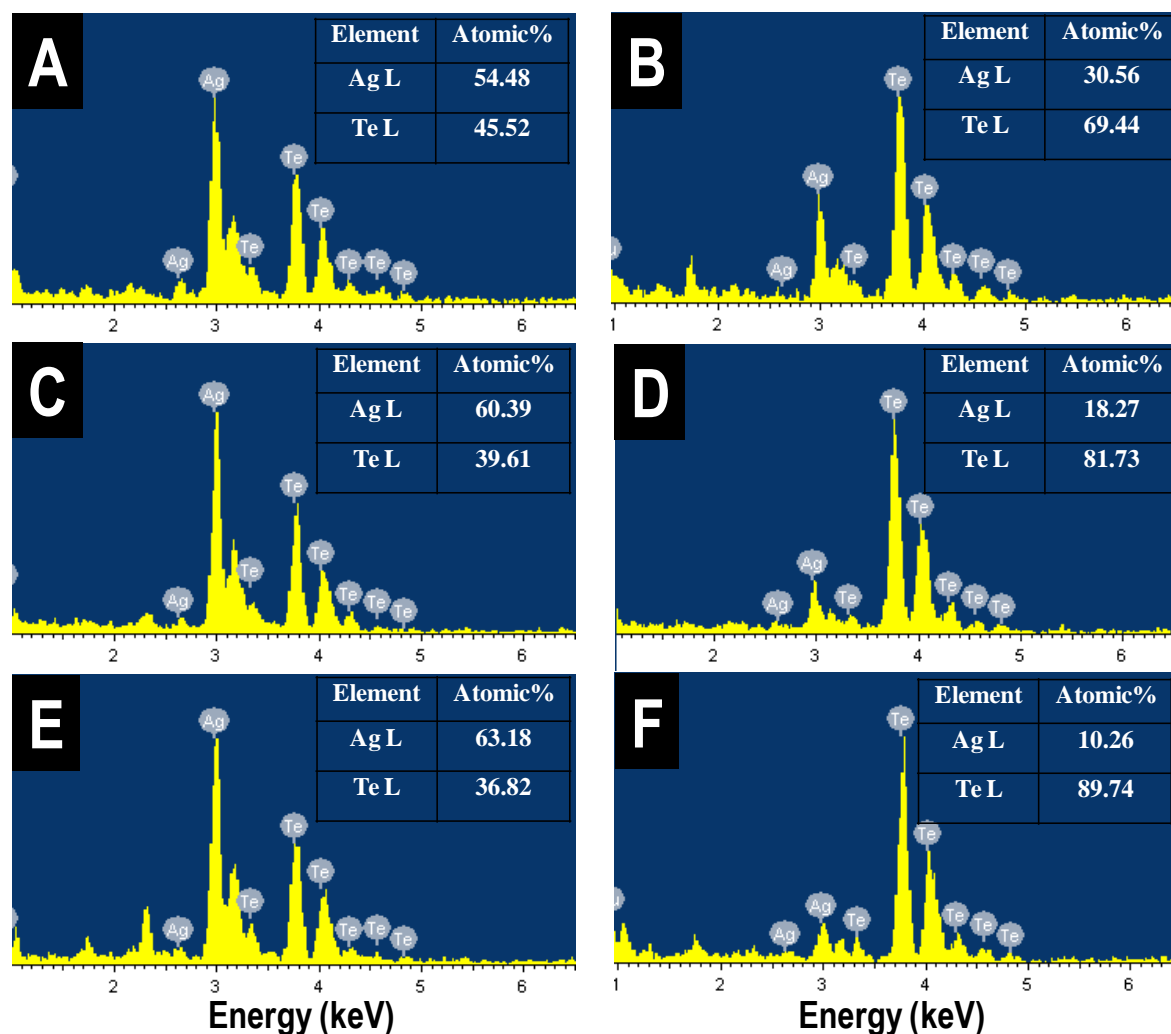
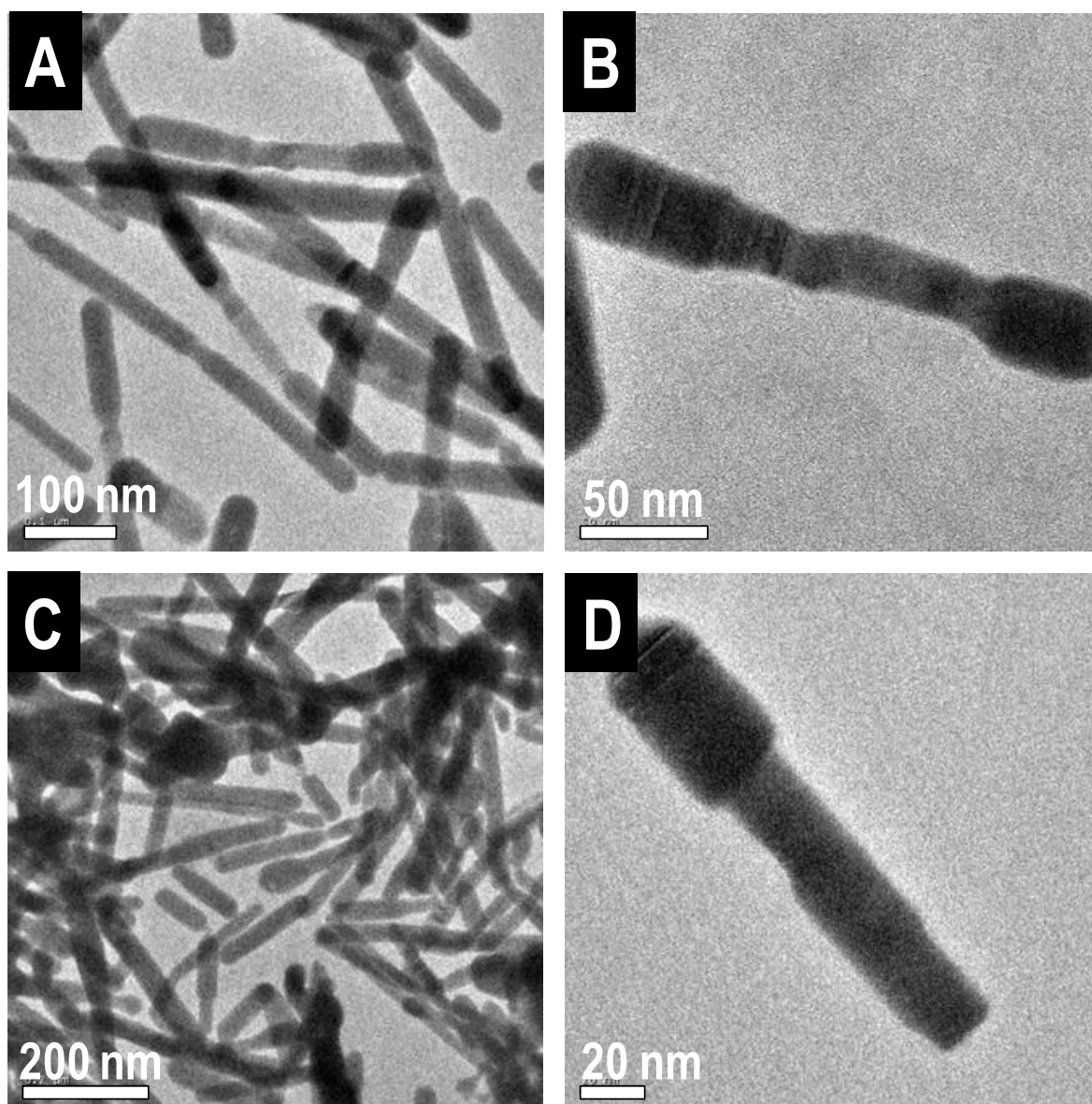


**Fig. S8** EDS spectra showing changes silver concentration at the tip and the middle section of the NWs during the annealing process. (A) Tip, after 6 h; (B) middle, after 6 h; (C) tip, after 12 h; (D) middle, after 12 h; (E) tip, after 18 h and (F) middle, after 18 h. Ag:Te atomic ratios are given in the tables. While the tips become silver rich with annealing time, the middle section become depleted in silver.

### S9. Supporting information 9



I

**Figure S9.** Bending and breaking observed in nanowires upon further annealing, once  $\text{Ag}_2\text{Te}-\text{Te}-\text{Ag}_2\text{Te}$  nanowire is formed after 24 hours. (A) Large area TEM image taken from sample annealed for 36 h. (B) TEM image of a single nanowire after 36 h of annealing. (C) Large area image showing the presence of broken nanowires after 48 hours of annealing. (D) TEM image of a single broken nanowire after 48 h.

## S10. Supporting information 10

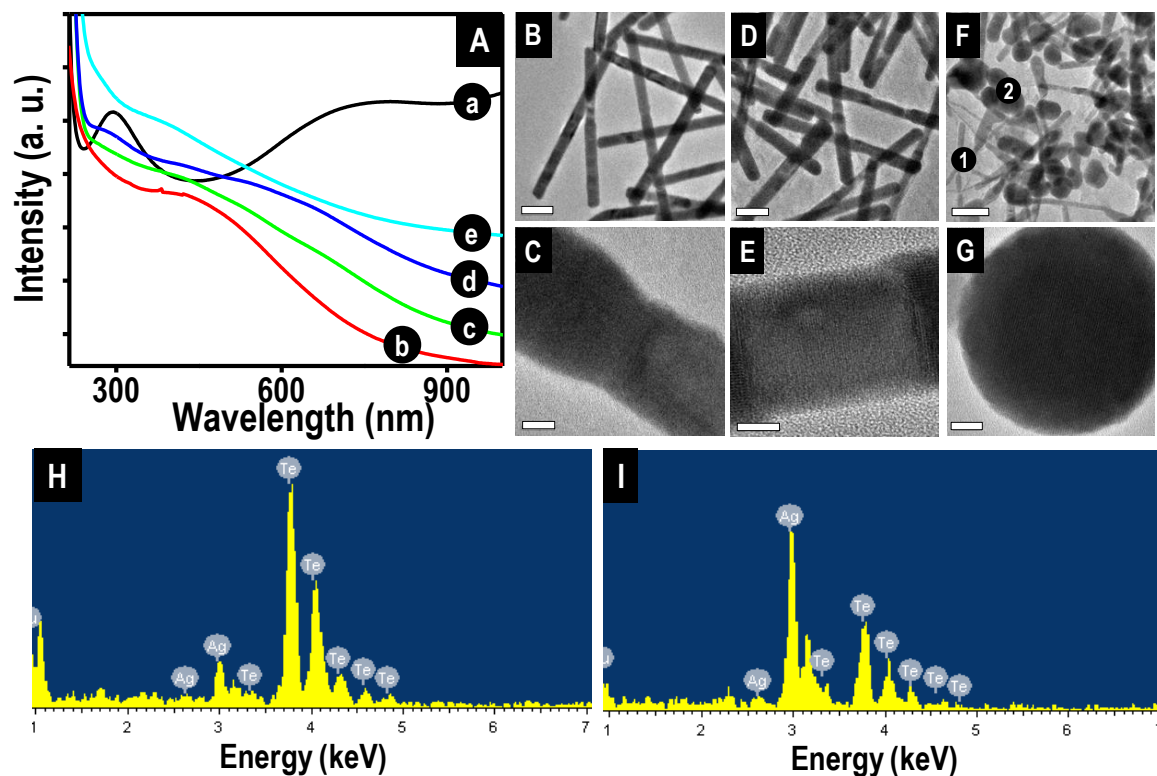


**Figure S10.** Effect of annealing temperature on nanowire morphology. (A) Traces c, d, e represent UV-visible extinction spectra for the partially silver reacted Te nanowires annealed at 50°, 70° and 90°C for 24 h. Traces a and b are spectra for Te and Ag<sub>2</sub>Te nanowires. Large area and high magnification TEM images of nanowires obtained after 24 h of annealing at different temperatures; (B,C) 50°C, (D,E) 70°C and (F,G) 90°C. Scale bars in large area and high magnification TEM images are 100 and 10 nm, respectively. (H) and (I) represent the EDS spectrum taken from areas 1 and 2 in image (F), respectively.

### S11. Supporting information 11

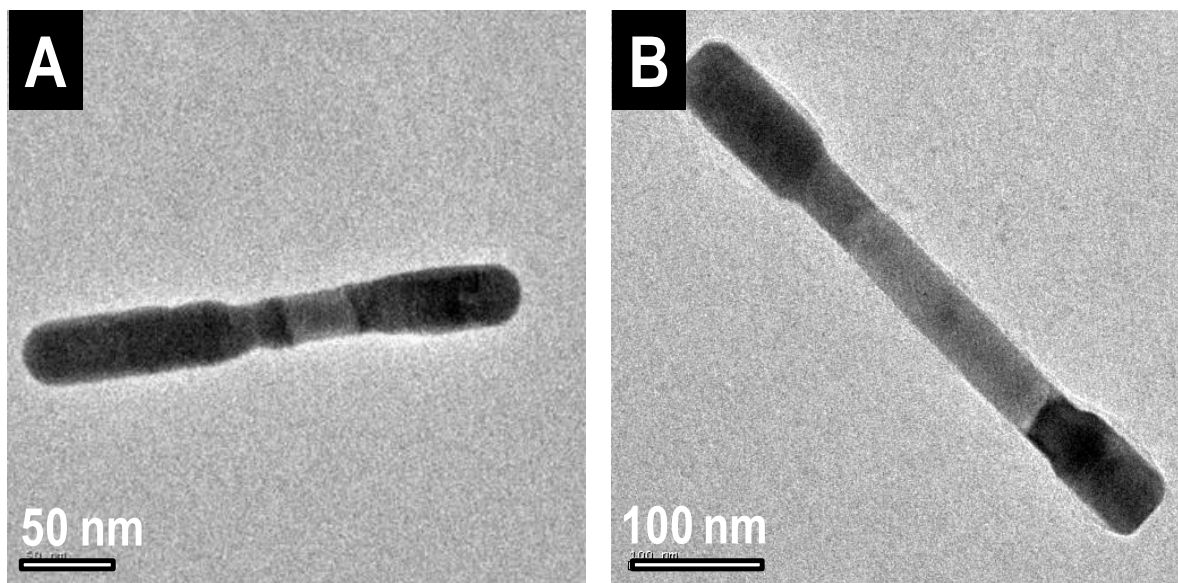


**Fig. S11** Tuning the length of Te and  $\text{Ag}_2\text{Te}$  sections. (A) NW with large  $\text{Ag}_2\text{Te}$  sections obtained by annealing of NWs with Ag:Te ratio greater than 1. (B) NW with small  $\text{Ag}_2\text{Te}$  sections obtained by annealing of NWs with a Ag:Te ratio less than 1.